Mechanics of Advanced Composite Structures 5 (2018) 13–24

Mechanics of Advanced Composite Structures

Journal homepage: http://MACS.journals.semnan.ac.ir

Semnan University

Bending, buckling and free vibration responses of hyperbolic shear deformable FGM beams

A.S. Sayyad[a*], Y.M. Ghugal[b]

[a] *Department of Civil Engineering, SRES's Sanjivani College of Engineering, Savitribai Phule Pune University, Kopargaon-423601, Maharashtra, India*
[b] *Department of Applied Mechanics, Government College of Engineering, Karad-415124, Maharashtra, India*

PAPER INFO

Paper history:
Received 2017-08-10
Revised 2017-12-25
Accepted 2018-01-16

Keywords:
Hyperbolic shear deformation theory
FGM beam
Bending
Buckling
Vibration

ABSTRACT

This study investigated bending, buckling, and free vibration responses of hyperbolic shear deformable functionally graded (FG) higher order beams. The material properties of FG beams are varied through thickness according to power law distribution; here, the FG beam was made of aluminium/alumina, and the hyperbolic shear deformation theory was used to evaluate the effect of shear deformation in the beam. The theory explains the hyperbolic cosine distribution of transverse shear stress through the thickness of a beam and satisfies zero traction boundary conditions on the top and bottom surfaces without requiring a shear correction factor. Hamilton's principle was employed to derive the equations of motion, and analytical solutions for simply supported boundary conditions were obtained using Navier's solution technique. The non-dimensional displacements, stress, natural frequencies, and critical buckling loads of FG beams were obtained for various values of the power law exponent. The numerical results were compared to previously published results and found to be in excellent agreement with these.

1. Introduction

Fibrous composite laminated beams are often subjected to delamination and stress concentration problems. This leads to the development of beams made of functionally graded materials (FGMs). A FGM is formed by varying the microstructure from one material to another in a specific gradient. The most commonly used FGMs are ceramic and metal for application in many engineering industries. Some typical practical applications for FGMs are given below.

1) Nuclear Projects: Fuel pellets and plasma walls of fusion reactors
2) Aerospace and Aeronautics: Stealth aircraft, rocket components, space plane frames, and space vehicles
3) Civil Engineering: Building materials, structural elements, and window glass
4) Defense: Armor plates and bullet-proof vests
5) Manufacturing: Machine tools, forming and cutting tools, metal casting, and forging processes
6) Energy Sector: Thermoelectric generators, solar cells and sensors

Detailed descriptions of applications of FGMs in various fields were presented by Koizumi [1, 2], Muller et al. [3], Pompe et al. [4], and Schulz et al. [5]. Increased use of beams, plates, and shells made of FGMs has led to the development of various analytical and numerical models for predicting accurate static bending, elastic buckling, and free vibration responses in these beams. Few studies have addressed the development of elasticity solutions for the analysis of FG beams, but those that have include Sankar [6], Zhong and Yu [7], Daouadji et al. [8], Ding et al. [9], Huang et al. [10], Ying et al. [11], Chu et al. [12], and Xu et al. [13].

Two-dimensional elasticity solutions are analytically difficult and computationally

* Corresponding author. Tel.: +91-9763567881

E-mail address: attu_sayyad@yahoo.co.in

cumbersome. Therefore, various approximate beam theories have been developed to analyze FG beams. Recently, Sayyad and Ghugal [14, 15] presented a comprehensive literature survey on various analytical and numerical methods for the analysis of isotropic and anisotropic beams and plates using displacement-based shear deformation theories. Similarly, Carrera et al. [16] presented recent developments in refined beam theories and related applications.

Since the effect of shear deformation is more pronounced in thick beams made of advanced composite materials, such as FGMs, classical beam theory (CBT) [17, 18] and first-order shear deformation theory [19] are not suitable for the analysis of thick FG beams. Therefore, higher order shear deformation theories are preferable for accurate analysis of FG thick beams. Various higher order shear deformation theories have been developed by various researchers for the analysis of isotropic and anisotropic beams, such as those by Reddy [20], Soldatos [21], Touratier [22], Karama et al. [23], Mantari et al. [24, 25], Neves et al. [26, 27], Sayyad and Ghugal [28, 29], Sayyad et al. [30, 31], Carrera et al. [32], Zenkour [33], Carrera and Ginuta [34], Carrera et al. [35], and Giunta et al. [36]. Such theories address bending, buckling, and free vibration analyses of beams using Carrera's unified formulation.

Thai and Vo [37] obtained Navier-type analytical solutions for the bending and vibration of FG beams using various higher order shear deformation theories. Li and Batra [38] obtained the critical buckling load of FG beams in various boundary conditions using the first-order shear deformation theory and CBT. Simsek [39] presented free vibration analysis of FG beams with various boundary conditions based on higher order shear deformation theories. Nguyen et al. [40] presented a Navier-type closed form solution for the static deformation and free vibration of FG beams using the first-order shear deformation theory. Hadji et al. [41, 42] developed new first-order and higher order shear deformation models for static and free vibration analysis of simply supported FG beams. Bourada et al. [43] presented a trigonometric shear and normal deformation theory that considers the effects of transverse shear and normal deformations for the analysis of FG higher order beams. The theory included three unknowns, one of which was the effect of the transverse normal. Vo et al. [44, 45] presented static bending and free vibration analysis based on higher order shear deformation theories using the finite element method. Recently, Sayyad and Ghugal [46] developed a unified shear deformation theory for the bending of FG beams and plates. Hebali et al. [47] developed five variable quasi-three-dimensional hyperbolic shear deformation theories for static and free vibration behavior of FG plates. Bennoun et al. [48] also developed five new variable shear and normal deformation plate theories for free vibration analysis of FG sandwich plates. Beldjelili et al. [49] investigated hygro-thermo-mechanical bending behavior of sigmoid FG plates resting on elastic foundations using four variable trigonometric shear deformation theories. Bouderba et al. [50] developed a simple first-order shear deformation theory for thermal buckling responses of FG sandwich plates to various boundary conditions. Bousahla et al. [51] also developed a four-variable refined plate theory for buckling analysis of FG plates subjected to uniform, linear, and non-linear temperature increases for various thicknesses. Boukhari et al. [52] developed a four-variable refined plate theory for wave propagation analysis of an infinite FG plate in thermal environments. Rahmani and Pedram [53] applied Timoshenko beam theory for free vibration analysis of FG nanobeams. Akgoz and Civalek [54] studied the static bending response of single-walled carbon nanotubes embedded in an elastic medium using higher-order shear deformation microbeams and a modified strain gradient theory. Ebrahimi and Barati [55] obtained a Navier-type solution for free vibration characteristics of FG nanobeams based on the third-order shear deformation beam theory.

In this paper, bending, buckling, and free vibration responses of hyperbolic shear deformable FG higher order beams were studied using the hyperbolic shear deformation theory of Soldatos [21]. Soldatos suggested using the hyperbolic function in the modeling and analysis of composite beams and plates in 1992, recommending that the hyperbolic function yields more accurate predictions of stress, frequencies, and the buckling loads of composite beams and plates. Since then, many researchers have used this function for the analysis of isotropic, laminated, and sandwich beams and plates. However, most research has not focused on the application of this function to evaluate the response of FG beams. Instead, researchers have applied hyperbolic shear deformation theory to bending, buckling, and free vibration analysis of FG beams.

The material properties of FG beams are varied through the thickness of the beam according to power law distribution. Here, the FG beam was made of aluminum (Al)/alumina (Al_2O_3), and the hyperbolic cosine distribution of transverse shear stress through the thickness of the beam satisfied the zero traction boundary conditions on the top and bottom surfaces without using the shear correction factor. The variationally consistent governing differential equations and boundary conditions of the theory were obtained using Hamilton's principle,

and an analytical solution for simply supported boundary conditions was obtained using Navier's solution. The non-dimensional displacements, stress, natural frequencies, and critical buckling loads of FG beams were obtained for various values of the power law exponent. The numerical results were then compared to previously published results and were in excellent agreement with these.

2. Variational formulation

2.1 Kinematics

Consider a FG beam with length ***L***, width ***b***, and thickness ***h*** made of Al/Al_2O_3 as shown in Figure 1. The bottom surface of the FG beam was ceramic-rich and top surface was metal-rich. The beam occupied the region $0 \le x \le L$; $-b/2 \le y \le b/2$; $-h/2 \le z \le h/2$ in the Cartesian coordinate systems. The *x*-axis was coincident with the beam neutral axis. The *z*-axis was assumed to be downward positive, and the beam was assumed to be deformed in the *x*-*z* plane only.

The mathematical formulation of the FG beam was based on the following kinematical assumptions.

1) The axial displacement ***u*** consists of the extension, bending, and shear components as
$$u(x,z) = u_{\text{extention}} + u_{\text{bending}} + u_{\text{shear}} \quad , \tag{1}$$
where
$$u_{\text{extention}} = u_0(x), \quad u_{\text{bending}} = -z\frac{dw_0(x)}{dx}, \quad u_{\text{shear}} = \left[z\cosh(1/2) - h\sinh(z/h)\right]\phi(x) \quad . \tag{2}$$
2) There is no relative motion in the *y*-direction at any point in the cross section of the beam.
3) Transverse displacement is assumed to be a function of the *x*-coordinate only.
$$w = w_0(x) \tag{3}$$
4) The theory applies to the hyperbolic cosine distribution of transverse shear stress through the thickness of the beam and satisfies zero traction boundary conditions on the top and bottom surfaces of the beam.
5) The axial displacement, ***u***, is such that the resultant axial stress (σ_x), acting over the cross-section, should result only in a bending moment and should not result in force in the *x*-direction.
6) Displacements are small, compared to beam thickness.
7) One-dimensional constitutive law is used to obtain stress values

Based on these assumptions, the displacement field of the hyperbolic shear deformation theory is given by:
$$u(x,z) = u_0 - z\frac{dw_0}{dx} + f(z)\phi, \quad w(x) = w_0(x) \quad , \quad f(z) = \left[z\cosh(1/2) - h\sinh(z/h)\right] \tag{4}$$

where u_0 is the axial displacement of a point on the neutral axis of the beam, w_0 is the transverse displacement of a point on the neutral axis of the beam, and the hyperbolic function is assumed according to the transverse shearing strain distribution across the thickness of the beam (see Figures 2 and 3). The nonzero normal and shear strains at any point of the beam are
$$\varepsilon_x = \frac{du_0}{dx} - z\frac{d^2w_0}{dx^2} + f(z)\frac{d\phi}{dx}, \quad \gamma_{zx} = f'(z)\phi \tag{5}$$
$$f'(z) = \left[\cosh(1/2) - \cosh(z/h)\right]$$

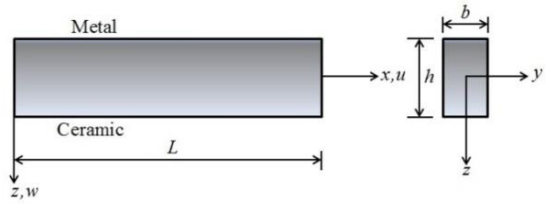

Figure 1. FG beam under bending conditions in the *x*-*z* plane

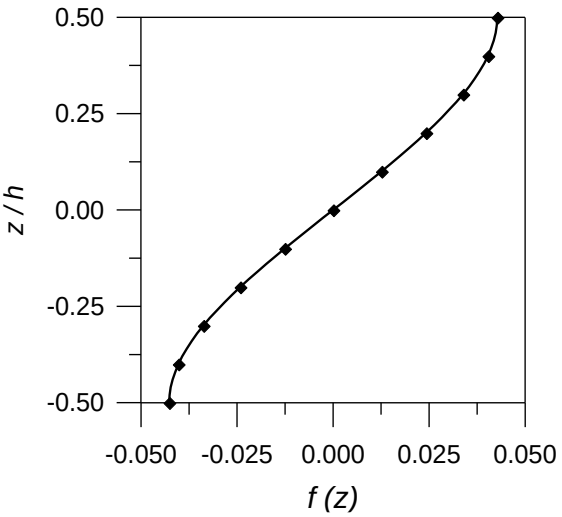

Figure 2. Through thickness distribution of the transverse shearing strain function

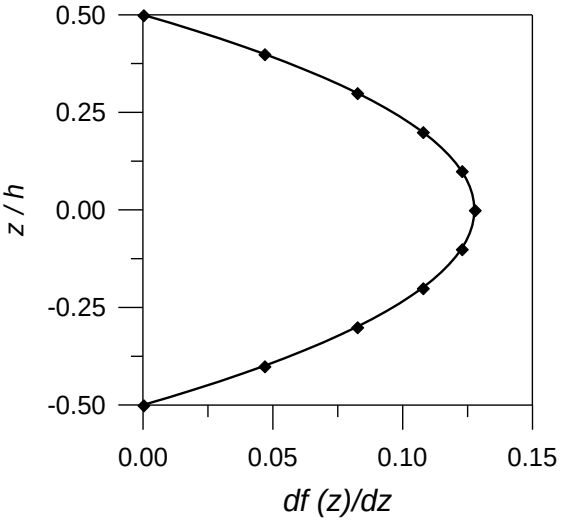

Figure 3. Through thickness distribution of the derivative of transverse shearing strain function

2.2 Constitutive relations

The FG beam was made of Al/Al_2O_3, and the properties of the material varied continuously throughout beam thickness, according to the power law distribution given by Equation (6).

$$\begin{aligned} E(z) &= E_m + (E_c - E_m)V_c, \\ G(z) &= G_m + (G_c - G_m)V_c \\ \rho(z) &= \rho_m + (\rho_c - \rho_m)V_c, \\ V_c &= \left[(1/2) + (z/h)\right]^p \end{aligned} \tag{6}$$

where ***E*** represents the Young's modulus, ***G*** represents the shear modulus, $\boldsymbol{\mu}$ represents the Poisson's ratio, and $\boldsymbol{\rho}$ represents mass density. Subscripts ***m*** and ***c*** represent the metallic and ceramic constituents, respectively, and ***p*** is the power law exponent. The variation of the Young's modulus ***E(z)*** through the thickness ***z/h*** of the beam for various values of the power law exponent is shown in Figure 4. The stress–strain relationship at any point of the beam is given by one-dimensional Hooke's law as follows.

$$\sigma_x = E(z)\varepsilon_x \quad \text{and} \quad \tau_{zx} = G(z)\gamma_{zx} \tag{7}$$

3. Equations of motion

Equations of motion of hyperbolic shear deformable FG beam are derived using Hamilton's principle,

$$\int_{t_1}^{t_2} (\delta U - \delta V + \delta K)\,dt = 0\ , \tag{8}$$

where $\delta U, \delta V$ and δK denotes variations in total strain energy, potential energy, and kinetic energy respectively, and t_1 and t_2 are the lower and upper limits of desired time period, respectively.

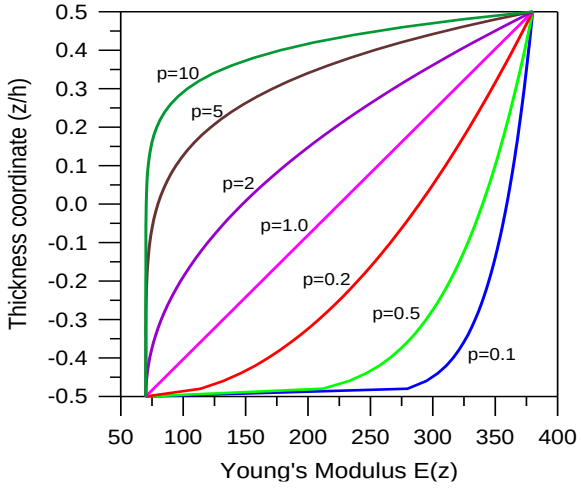

Figure 4. Variation in Young's modulus $E(z)$ through the thickness of the FG beam for various values of the power law exponent (p)

The variation of the strain energy (δU) can be stated as:

$$\begin{aligned} \delta U &= \int_0^L \int_{-b/2}^{b/2} \int_{-h/2}^{h/2} (\sigma_x \delta\varepsilon_x + \tau_{zx}\delta\gamma_{zx})\,dz\,dy\,dx \\ &= \int_0^L \left(N_x \frac{d\delta u_0}{dx} - M^c \frac{d^2\delta w_0}{dx^2} + M^s \frac{d\delta\phi}{dx} + Q\delta\phi \right) dx \end{aligned}\ , \tag{9}$$

where N_x, M^c, M^s and Q are the axial force, bending moment, higher order moment, and shear force resultants, respectively. Additionally,

$$\begin{aligned} N_x &= b\int_{-h/2}^{h/2} \sigma_x\,dz = A\frac{du_0}{dx} - B\frac{d^2w_0}{dx^2} + C\frac{d\phi}{dx} \\ M^c &= b\int_{-h/2}^{h/2} \sigma_x\, z\,dz = B\frac{du_0}{dx} - D\frac{d^2w_0}{dx^2} + E\frac{d\phi}{dx} \\ M^s &= b\int_{-h/2}^{h/2} \sigma_x\, f(z)\,dz = C\frac{du_0}{dx} - E\frac{d^2w_0}{dx^2} + \\ & F\frac{d\phi}{dx} \\ Q &= b\int_{-h/2}^{h/2} \tau_{zx}\, f'(z)\,dz = H\phi \end{aligned}\ , \tag{10}$$

where

$$\begin{aligned} &A = b\int_{-h/2}^{h/2} E(z)\,dz,\ B = b\int_{-h/2}^{h/2} E(z)\,z\,dz, \\ &C = b\int_{-h/2}^{h/2} E(z)\,f(z)\,dz, \\ &D = b\int_{-h/2}^{h/2} E(z)\,z^2\,dz, \\ &E = b\int_{-h/2}^{h/2} E(z)\,z\,f(z)\,dz, \\ &F = b\int_{-h/2}^{h/2} E(z)\left[f(z)\right]^2 dz, \\ &H = b\int_{-h/2}^{h/2} G(z)\left[f'(z)\right]^2 dz \end{aligned} \tag{11}$$

The variation of the potential energy (δV) due to transverse and axial loads can be written as

$$\delta V = \int_0^L \left(q\delta w + N_0 \frac{dw}{dx}\frac{d\delta w}{dx} \right) dx\ . \tag{12}$$

The variation of kinetic energy (δK) can be written in following form

$$\begin{aligned} \delta K &= \int_0^L \int_{-b/2}^{b/2} \int_{-h/2}^{h/2} \rho(z)(\ddot{u}\delta u + \ddot{w}\delta w)\,dz\,dy\,dx \\ &= \int_0^L \left(I_A\ddot{u}_0 - I_B\frac{d\ddot{w}_0}{dx} + I_C\ddot{\phi} \right)\delta u_0\,dx \\ &+ \int_0^L \left(-I_B\ddot{u}_0 + I_D\frac{d\ddot{w}_0}{dx} - I_E\ddot{\phi} \right)\frac{d\delta w_0}{dx}\,dx \\ &+ \int_0^L \left(I_C\ddot{u}_0 - I_E\frac{d\ddot{w}_0}{dx} + I_F\ddot{\phi} \right)\delta\phi\,dx \\ &+ \int_0^L (I_A\ddot{w}_0)\delta w_0\,dx \end{aligned}\ , \tag{13}$$

where $\rho(z)$ is the mass density, and $I_A, I_B, I_C, I_D, I_E, I_F$ are the inertia coefficients.

$$\begin{aligned} I_A &= b\int_{-h/2}^{h/2}\rho(z)\,dz, \\ I_B &= b\int_{-h/2}^{h/2}\rho(z)\,z\,dz, \\ I_C &= b\int_{-h/2}^{h/2}\rho(z)\,f(z)\,dz, \\ I_D &= b\int_{-h/2}^{h/2}\rho(z)\,z^2\,dz, \\ I_E &= b\int_{-h/2}^{h/2}\rho(z)\,z\,f(z)\,dz, \\ I_F &= b\int_{-h/2}^{h/2}\rho(z)\left[f(z)\right]^2 dz \end{aligned} \tag{14}$$

Substituting Equations (9), (12), and (13) into Equation (8), doing the integrations and setting the coefficients of δu_0, δw_0, and $\delta\phi$ to equal zero, the following equations of motion are obtained.

$$\begin{aligned} &\frac{dN_x}{dx} = I_A\ddot{u}_0 - I_B\frac{d\ddot{w}_0}{dx} + I_C\ddot{\phi} \\ &\frac{d^2M^c}{dx^2} = -q + N_0\frac{d^2w_0}{dx^2} \\ &\qquad + I_B\frac{d\ddot{u}_0}{dx} - I_D\frac{d^2\ddot{w}_0}{dx^2} + I_A\ddot{w}_0 + I_E\frac{d\ddot{\phi}}{dx} \\ &\frac{dM^s}{dx} - Q = I_C\ddot{u}_0 - I_E\frac{d\ddot{w}_0}{dx} + I_F\ddot{\phi} \end{aligned} \tag{15}$$

By substituting the stress resultants from Equation (10) into Equation (15), the following equations of motion can be obtained for unknown displacement variables.

$$\begin{aligned} &A\frac{d^2u_0}{dx^2} - B\frac{d^3w_0}{dx^3} + C\frac{d^2\phi}{dx^2} \\ &\qquad = I_A\ddot{u}_0 - I_B\frac{d\ddot{w}_0}{dx} + I_C\ddot{\phi} \\ &B\frac{d^3u_0}{dx^3} - D\frac{d^4w_0}{dx^4} + E\frac{d^3\phi}{dx^3} = -q + N_0\frac{d^2w_0}{dx^2} \\ &\qquad + I_B\frac{d\ddot{u}_0}{dx} - I_D\frac{d^2\ddot{w}_0}{dx^2} + I_A\ddot{w}_0 + I_E\frac{d\ddot{\phi}}{dx} \\ &C\frac{d^2u_0}{dx^2} - E\frac{d^3w_0}{dx^3} + F\frac{d^2\phi}{dx^2} - H\phi \\ &\qquad = I_C\ddot{u}_0 - I_E\frac{d\ddot{w}_0}{dx} + I_F\ddot{\phi} \end{aligned} \tag{16}$$

4. Analytical solution

Consider a simply supported FG beam with length '*L*' and rectangular cross-section '*b*×*h*'. For simply supported boundary conditions, according to Navier's solution, the unknown displacement variables are expanded in a Fourier series as given below:

$$\begin{aligned} u_0 &= \sum_{m=1,3,5}^{\infty} u_m\cos\alpha x\; e^{i\omega t}, \\ w_0 &= \sum_{m=1,3,5}^{\infty} w_m\sin\alpha x\; e^{i\omega t}, \\ \phi &= \sum_{m=1,3,5}^{\infty} \phi_m\cos\alpha x\; e^{i\omega t} \end{aligned} \tag{17}$$

where $i=\sqrt{-1}$, $\alpha = m\pi/L$, and (u_m, w_m, ϕ_m) are the unknown coefficients, and ω is the natural frequency. The uniform transverse load (q) acting on the top surface of the beam was also expanded in the Fourier series as

$$q = \sum_{m=1,3,5}^{\infty}\frac{4q_0}{m\pi}\sin\alpha x, \tag{18}$$

where q_0 is the maximum intensity of the load at the center of the beam. By substituting Equations (17) and (18) into Equation (16), the analytical solution can be obtained from the following equations.

For bending, ignore time derivatives and axial force.

$$\begin{bmatrix} A\alpha^2 & -B\alpha^3 & C\alpha^2 \\ -B\alpha^3 & D\alpha^4 & -E\alpha^3 \\ C\alpha^2 & -E\alpha^3 & F\alpha^2+H \end{bmatrix}\times\begin{Bmatrix} u_m \\ w_m \\ \phi_m \end{Bmatrix} = \begin{Bmatrix} 0 \\ 1 \\ 0 \end{Bmatrix}\frac{4q_0}{m\pi}. \tag{19}$$

For buckling, ignore time derivatives and transverse load.

$$\left\{\begin{bmatrix} A\alpha^2 & -B\alpha^3 & C\alpha^2 \\ -B\alpha^3 & D\alpha^4 & -E\alpha^3 \\ C\alpha^2 & -E\alpha^3 & F\alpha^2+H \end{bmatrix} - N_0\begin{bmatrix} 0 & 0 & 0 \\ 0 & \alpha^2 & 0 \\ 0 & 0 & 0 \end{bmatrix}\right\} \times\begin{Bmatrix} u_m \\ w_m \\ \phi_m \end{Bmatrix} = \begin{Bmatrix} 0 \\ 0 \\ 0 \end{Bmatrix}, \tag{20}$$

For free vibrations, ignore transverse load and axial force.

$$\begin{bmatrix} A\alpha^2 & -B\alpha^3 & C\alpha^2 \\ -B\alpha^3 & D\alpha^4 & -E\alpha^3 \\ C\alpha^2 & -E\alpha^3 & F\alpha^2+H \end{bmatrix}\times\begin{Bmatrix} u_m \\ w_m \\ \phi_m \end{Bmatrix} - \omega^2\begin{bmatrix} I_A & -I_B\alpha & I_C \\ -I_B\alpha & (I_D\alpha^2+I_A) & -I_E\alpha \\ I_C & -I_E\alpha & I_F \end{bmatrix}\times\begin{Bmatrix} u_m \\ w_m \\ \phi_m \end{Bmatrix} = \begin{Bmatrix} 0 \\ 0 \\ 0 \end{Bmatrix}. \tag{21}$$

5. Numerical results and discussion

In this section, the accuracy of hyperbolic shear deformation theory for predicting bending, buckling, and vibration responses of FG higher order beams was investigated. The numerical results were obtained using Navier's solution for simply supported boundary conditions. The beam was made of Al_2O_3 for ceramic (E_c = 380 GPa, ρ_c =3960 kg/m^3, μ = 0.3) and Al for metal (E_m = 70 GPa, ρ_m =2702

kg/m^3, μ = 0.3). The material properties of the beam were varied across beam thickness according to power law distribution. The bottom surface of the FG beam was ceramic-rich, and the top surface was metal-rich.

5.1 Bending the FG beam

The bending response of the FG beam under a uniform transverse load was investigated. The displacements and stress are presented in the following non-dimensional form.

Axial displacement (u) at x = 0 and z = -h/2:

$$\bar{u} = \frac{u100E_m h^3}{q_0 L}.$$

Transverse displacement (w) at x = L/2 and z = 0:

$$\bar{w} = \frac{w100E_m h^3}{q_0 L}.$$

Axial stress (σ_x) at x = L/2 and z = h/2:

$$\bar{\sigma}_x = \frac{\sigma_x h}{q_0 L}.$$

Transverse shear stress (τ_{xz}) at x = 0 and z = 0:

$$\bar{\tau}_{xz} = \frac{\tau_{xz} h}{q_0 L}.$$

The numerical results obtained using the present theory were compared to those of other theories, which is shown in Table 1. Comparisons of numerical results are presented in Table 2. Through thickness distribution of displacements and stress are shown in Figure 5 (a–c). The displacements and stress are presented for various values of the power law exponent (p). The transverse shear stress was evaluated directly from constitutive relations. The present results were compared to higher order shear deformation theories of Reddy [20], Touratier [22], and Hadji et al. [42] and the CBT. The present results were in good agreement with those obtained using various shear deformation theories for all values of the power law exponent. Because the effect of transverse shear deformation is not included in the CBT, this theory underestimated displacement and stress. The stress presented by Hadji et al. [42] was higher compared to that obtained using shear deformation theories. The present theory gives a linear variation of axial stress $(\bar{\sigma}_x)$ through the thickness for p = 0 and p = ∞; however, for other values of the power law exponent, this is non-linear through the thickness (see Figure 5b). Displacements and stress are increased as the power law exponent increases, creating more flexibility in FG beams.

Table 1. Displacement fields of the present and referred theories

Reference	Displacement field
Present	$f(z) = \left[z\cosh\left(\frac{1}{2}\right) - h\sinh\left(\frac{z}{h}\right) \right]$
Hadji et al. [42]	$f(z) = \frac{1}{\lambda}\left[\frac{3}{2}\left(\frac{z}{h}\right) - 2\left(\frac{z}{h}\right)^3 \right]$
Reddy [20]	$f(z) = z\left[1 - \frac{4}{3}\left(\frac{z^2}{h^2}\right) \right]$
Touratier [22]	$f(z) = \frac{h}{\pi}\sin\frac{\pi z}{h}$
TBT	$f(z) = z$
CBT	$f(z) = 0$

Figure 5(b) shows that an increase in the power law exponent increased the compression zone in the beam, while Figure 5(c) shows the hyperbolic cosine variation of transverse shear stress $(\bar{\tau}_{zx})$ that was across the thickness of the beam and that satisfied the traction free conditions at the top and bottom surfaces of the beam. Figure 5(c) also shows an increase in the power law exponent neutral axis that shifted toward the bottom. This was due to ceramic, with which metal has a low elastic modulus.

5.2 Buckling an FG beam

In this section, the buckling response of an FG beam subjected to axial force (N_0) was investigated. A non-dimensional critical buckling load is presented in Table 3. The non-dimensional form of the buckling load was as follows:

$$\bar{N}_{cr} = \frac{12N_0 a^2}{E_m h^3}.$$

The critical buckling load was obtained for various values regarding the power law exponent (p) and a length-to-thickness ratio (L/h). Results were compared with those presented by Li and Batra [38], Nguyen et al. [40], and Vo et al. [45]. Table 3 reveals that this study's results agreed with those available in the literature. Specifically, the critical buckling load was higher for a thin, slender beam and lower for a thick beam. However, the critical buckling load was in a non-dimensional form; non-dimensional quantities are reciprocal of dimensional quantities. According to Euler's buckling theory, critical buckling loads are directly proportional to cross-sections of beams (i.e., moments of inertia). Therefore, it can be noted that the dimensional critical buckling load for the slender beam was actually smaller than the load for the thicker beam.

Table 2. A comparison of the non-dimensional displacements and stress of the FG beams subjected to uniform loads with various power law exponent values

		L/h = 5				*L/h* = 20			
p	Theory	$\bar{u}$	$\bar{w}$	$\bar{\sigma}_x$	$\bar{\tau}_{zx}$	$\bar{u}$	$\bar{w}$	$\bar{\sigma}_x$	$\bar{\tau}_{zx}$
0	Present	0.9274	3.1224	3.7529	0.7259	0.2275	2.8585	14.8179	0.7259
	Hadji et al. [42]	0.9233	3.1673	3.9129	0.7883	0.2290	2.8807	15.4891	0.7890
	Reddy [20]	0.9397	3.1654	3.8019	0.7330	0.2306	2.8962	15.0129	0.7437
	Touratier [22]	0.9409	3.1649	3.8053	0.7549	0.2306	2.8962	15.0138	0.7686
	CBT	0.9211	2.8783	3.7500	-	0.2303	2.8783	15.0000	-
1	Present	2.2735	6.2586	5.8077	0.7187	0.5611	5.7292	22.9038	0.7259
	Hadji et al. [42]	2.2115	6.1805	6.0709	0.7883	0.5498	5.6965	24.0095	0.7890
	Reddy [20]	2.3036	6.2594	5.8836	0.7330	0.5686	5.5685	23.2051	0.7432
	Touratier [22]	2.3058	6.2586	5.8892	0.7549	0.5686	5.8049	23.2067	0.7686
	CBT	2.2722	5.7746	5.7959	-	0.5680	5.7746	23.1834	-
2	Present	3.0720	7.9627	6.7938	0.6573	0.7591	7.3450	26.7470	0.6648
	Hadji et al. [42]	2.9629	7.9106	7.0925	0.7274	0.7366	7.2458	27.9844	0.728
	Reddy [20]	3.1127	8.0677	6.8824	0.6704	0.7691	7.4421	27.0989	0.6812
	Touratier [22]	3.1153	8.0683	6.8901	0.6933	0.7692	7.4421	27.1010	0.7069
	CBT	3.0740	7.4003	6.7676	-	0.7685	7.4003	27.0704	-
5	Present	3.6612	9.6986	8.0059	0.5786	0.9014	8.7031	31.3997	0.5863
	Hadji et al. [42]	3.5429	9.6933	8.3581	0.6523	0.8775	8.6182	32.8183	0.6540
	Reddy [20]	3.7097	9.8281	8.1104	0.5904	0.9134	8.8182	31.8127	0.6013
	Touratier [22]	3.7140	9.8367	8.1222	0.6155	0.9134	8.8188	31.8159	0.6292
	CBT	3.6496	8.7508	7.9428	-	0.9124	8.7508	31.7711	-
10	Present	3.8351	10.7949	9.5870	0.6412	0.9412	9.5641	37.6432	0.6426
	Hadji et al. [42]	3.7462	10.8680	9.9878	0.7064	0.9262	9.5513	39.2717	0.7091
	Reddy [20]	3.8859	10.9381	9.7119	0.6465	0.9536	9.6905	38.1382	0.6586
	Touratier [22]	3.8913	10.9420	9.7238	0.6708	0.9537	9.6908	38.1414	0.6858
	CBT	3.8097	9.6072	9.5228	-	0.9524	9.6072	38.0913	-

5.3 *The free vibrations of FG beams*

The free vibration responses of FG beams were investigated. Fundamental frequencies were obtained for various power law exponent values and *L/h* ratios. The results were compared to those presented by Reddy [20], Simsek [39], Thai and Vo [37], Vo et al. [45], and Timoshenko [19] and those obtained with the CBT. Fundamental frequencies were presented in the following non-dimensional form:

$$\bar{\omega} = \left(\omega L^2 / h\right)\sqrt{\left(\rho_m / E_m\right)}\,.$$

Table 4 shows the non-dimensional fundamental frequencies ($\bar{\omega}$) of simply supported FG beams. The natural frequencies of first three bending modes are presented. Table 4 reveals that the fundamental frequencies obtained using the theory presented in this research were in excellent agreement with those obtained by other researchers. The numerical results showed that all shear deformation theories predicted more or less the same frequencies, whereas the CBT overestimated all frequencies due to a neglect of shear deformation. The effects of a power law exponent, *p*, on the frequencies of FG beams are shown in Figure 6(b). It was observed that increases in power law exponent values led to reductions of fundamental frequencies. This was because the increases in power law exponent values resulted in decreases in elasticity modulus values. It should be noted that the fundamental frequencies were higher when there were higher modes of vibration.

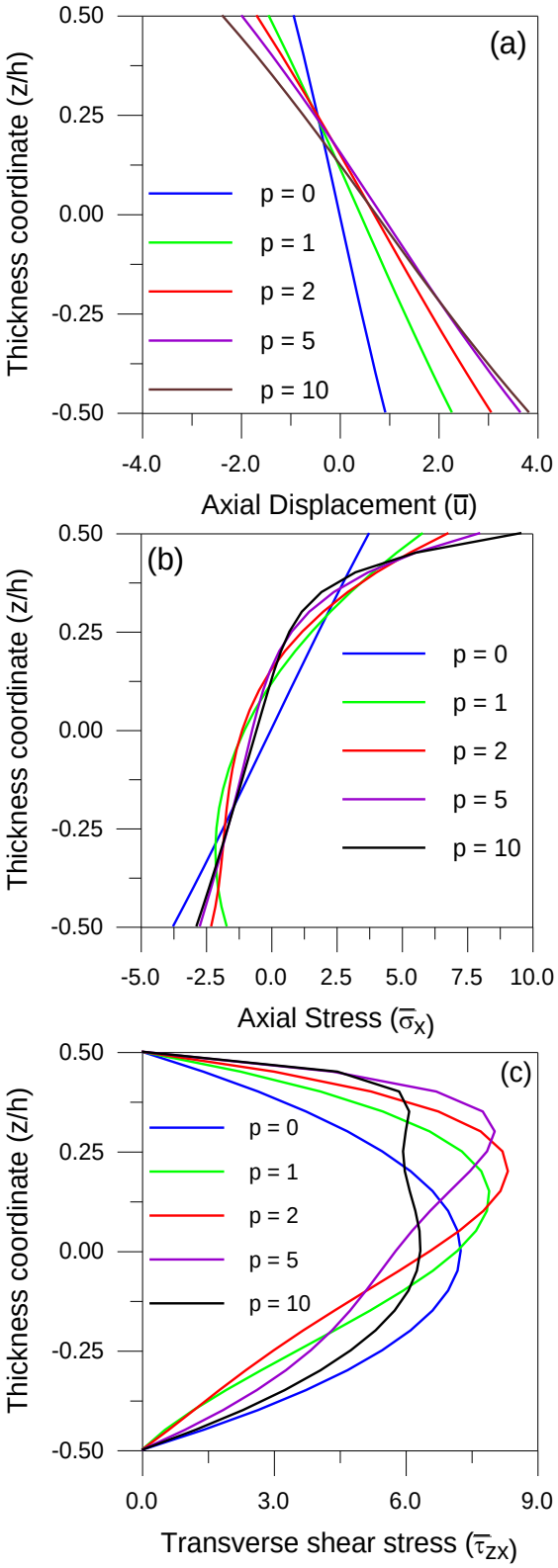

Figure 5. Through thickness distribution of the non-dimensional (a) axial displacement ($\bar{u}$), (b) the axial stress ($\bar{\sigma}_x$), and (c) transverse shear stress ($\bar{\tau}_{zx}$) simply supported the FG beam under a uniform load throughout various power law exponent values (L/h = 5)

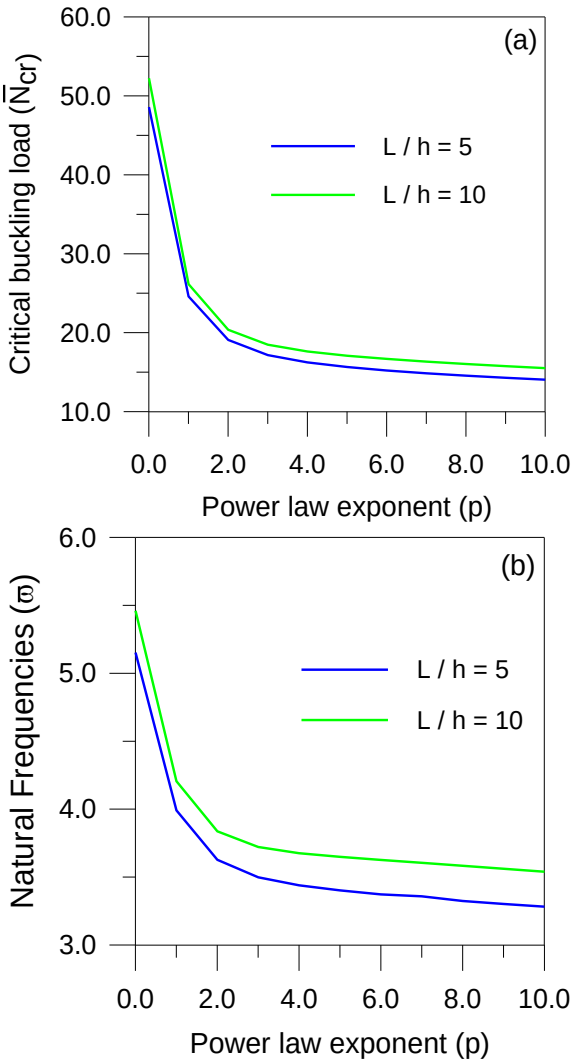

Figure 6. The variations in non-dimensional (a) critical buckling loads and (b) natural frequencies with respect to the power law exponents of simply supported FG beams.

Table 3. A comparison of the non-dimensional critical buckling loads ($\bar{N}_{cr}$) of the FG beams subjected to axial forces in regards to various power law exponent values

		p				
L/h	Theory	0	1	2	5	10
5	Present	48.596	24.584	19.071	15.645	14.052
	Li and Batra [38]	48.835	24.687	19.245	16.024	14.427
	Nguyen et al. [40]	48.835	24.687	19.245	16.024	14.427
	Vo et al. [45]	48.837	24.689	19.247	16.026	14.428
	Vo et al. [45]	48.840	24.691	19.160	16.740	14.146
10	Present	52.238	26.141	20.366	17.082	15.500
	Li and Batra [38]	52.309	26.171	20.416	17.192	15.612
	Nguyen et al. [40]	52.309	26.171	20.416	17.194	15.612
	Vo et al. [45]	52.308	26.172	20.418	17.195	15.613
	Vo et al. [45]	52.308	26.172	20.393	17.111	15.529

Table 4. A comparison of the first three non-dimensional fundamental frequencies of the FG beams in regards to various power law exponent values

			p				
L/h	Mode	Theory	0	1	2	5	10
5	1	Present	5.1527	3.9904	3.6264	3.4014	3.2816
		Reddy [20]	5.1527	3.9904	3.6264	3.4012	3.2816
		Simsek [39]	5.1527	3.9904	3.6264	3.4012	3.2816
		Thai and Vo [37]	5.1527	3.9904	3.6264	3.4012	3.2816
		Vo et al. [45]	5.1527	3.9716	3.5979	3.3742	3.2653
		Timoshenko [19]	5.1524	3.9902	3.6343	3.4311	3.3134
		CBT	5.3953	4.1484	3.7793	3.5949	3.4921
	2	Present	17.881	14.010	12.640	11.544	11.024
		Thai and Vo [37]	17.881	14.009	12.640	11.544	11.024
		CBT	20.618	15.798	14.326	13.587	13.237
	3	Present	34.202	27.098	24.316	21.720	20.556
		Thai and Vo [37]	34.208	27.097	24.315	21.718	20.556
		CBT	43.348	33.027	29.745	28.085	27.475
20	1	Present	5.4603	4.2050	3.8361	3.6485	3.5390
		Reddy [20]	5.4603	4.2050	3.8361	3.6485	3.5389
		Simsek [39]	5.4603	4.2050	3.8361	3.6485	3.5389
		Thai and Vo [37]	5.4603	4.2050	3.8361	3.6484	3.5389
		Vo et al. [45]	5.4603	4.2038	3.8342	3.6466	3.5378
		Timoshenko [19]	5.4603	4.2050	3.8367	3.6508	3.5415
		CBT	5.4777	4.2163	3.8472	3.6628	3.5547
	2	Present	21.573	16.634	15.161	14.374	13.926
		Thai and Vo [37]	21.573	16.634	15.161	14.374	13.926
		CBT	21.843	16.810	15.333	14.595	14.167
	3	Present	47.593	36.768	33.469	31.579	30.095
		Thai and Vo [37]	47.593	36.767	33.469	31.5789	30.537
		CBT	48.899	37.617	34.295	32.6357	31.688

6. Conclusions

A hyperbolic shear deformation theory developed by Soldatos [21] was extended in this paper to conduct bending, buckling, and free vibration analyses of FG beams. With the theory, hyperbolic cosine variations of transverse shear stress were found at the top and bottom surfaces of the beams. Subsequently, Hamilton's principle was employed to derive equations of motion. The equations of motion, with the theory, were variationally consistent and allowed the avoidance of a shear correction factor. Then, an analytical solution for a simply supported boundary condition was obtained using Navier's solution procedure.

The numerical results were compared to those obtained by other researchers to determine the accuracy of the theory. Based on the comparisons and a discussion, it was concluded that the displacements, stress, critical buckling loads, and natural frequencies obtained using the theory were accurate and in agreement with those obtained using other refined shear deformation theories. It was seen that varying material properties had significant effects on the dimensionless stress, frequencies, and buckling loads of the FG beams. Increasing power law exponent values reduced the stiffnesses of the FG

beams and consequently led to increases in displacements and reductions of frequencies and buckling loads. Overall, the investigation of the bending, buckling, and free vibration responses of the FG beams confirmed the effects and credibility of the hyperbolic shear deformation theory.

References

[1] Koizumi M. The concept of FGM, *Functionally Gradient Material*, 1993; 34: 3–10.

[2] Koizumi M. FGM activities in Japan. *Composites Part B*, 1997; 28: 1–4.

[3] Muller E, Drasar C, Schilz J, Kaysser WA. Functionally graded materials for sensor and energy applications. *Mater. Sci. Eng. A*, 2003; 362: 17–39.

[4] Pompe W, Worch H, Epple M, Friess W, Gelinsky M, Greil P, Hempele U, Scharnweber D, Schulte K. Functionally graded materials for biomedical applications. *Mater. Sci. Eng. A*, 2003; 362: 40–60.

[5] Schulz U, Peters M, Bach FW, Tegeder G. Graded coatings for thermal, wear and corrosion barriers. *Mater. Sci. Eng. A*, 2003; 362: 61–80.

[6] Sankar BV. An elasticity solution for functionally graded beams. *Compos Sci Technol.*, 2001; 61(5): 689–696.

[7] Zhong Z, Yu, T. Analytical solution of a cantilever functionally graded beam. *Compos Sci Technol.*, 2007; 67: 481–488.

[8] Daouadji TH, Henni AH, Tounsi A, Bedia EAA. Elasticity solution of a cantilever functionally graded beam. *Appl Compos Mater*, 2013; 20: 1–15.

[9] Ding JH, Huang DJ, Chen WQ. Elasticity solutions for plane anisotropic functionally graded beams. *Int J of Solids and Structures*, 2007; 44(1): 176–196.

[10] Huang DJ, Ding JH, Chen WQ. Analytical solution and semi-analytical solution for anisotropic functionally graded beam subject to arbitrary loading. *Science in China Series G*, 2009; 52(8): 1244-1256.

[11] Ying J, Lu CF, Chen WQ. Two-dimensional elasticity solutions for functionally graded beams resting on elastic foundations. *Composite Structures*, 2008; 84: 209–219.

[12] Chu P, Li XF, Wu JX, Lee KY. Two-dimensional elasticity solution of elastic strips and beams made of functionally graded materials under tension and bending. *Acta Mechanica*, 2015; 226: 2235–2253.

[13] Xu Y, Yu T, Zhou D. Two-dimensional elasticity solution for bending of functionally graded beams with variable thickness. *Meccanica*, 2014; 49: 2479–2489.

[14] Sayyad AS, Ghugal YM. On the free vibration analysis of laminated composite and sandwich plates: A review of recent literature with some numerical results. *Composite Structures*, 2015; 129: 177–201.

[15] Sayyad AS, Ghugal YM. Bending, buckling and free vibration of laminated composite and sandwich beams: A critical review of literature. *Composite Structures*, 2017**;** 171: 486–504.

[16] Carrera E, Pagani A, Petrolo M, Zappino E. Recent developments on refined theories for beams with applications. *Mechanical Engineering Reviews*, 2015; 2(2): 1-30.

[17] Bernoulli J. Curvatura laminae elasticae. *Acta Eruditorum Lipsiae*, 1694; 262 – 276.

[18] Euler L. Methodus inveniendi lineas curvas maximi minimive proprietate gaudentes. *Lausanne and Geneva,* 1744.

[19] Timoshenko SP. On the correction for shear of the differential equation for transverse vibrations of prismatic bars. *Philosophical Magazine*, 1921; 41(6): 742-746.

[20] Reddy JN. A simple higher order theory for laminated composite plates. *J of Applied Mechanics*, 1984; 51: 745–752.

[21] Soldatos KP. A transverse shear deformation theory for homogeneous monoclinic plates, *Acta Mechanica*, 1992; 94: 195–200.

[22] Touratier M. An efficient standard plate theory. *Int J Engineering Science*, 1991; 29: 901–916.

[23] Karama M, Afaq KS, Mistou S. Mechanical behavior of laminated composite beam by new multi-layered laminated composite structures model with transverse shear stress continuity. *Int J Solids and Structures*, 2003; 40: 1525–1546.

[24] Mantari JL, Oktem AS, Soares CG. A new higher order shear deformation theory for sandwich and composite laminated plates. *Composites Part B*, 2012; 43: 1489–1499.

[25] Mantari JL, Oktem AS, Soares CG. A new trigonometric shear deformation theory for isotropic, laminated composite and sandwich plates. *Int J Solids and Structures*, 2012; 49: 43–53.

[26] Neves AMA, Ferreira AJM, Carrera E, Roque CMC, Cinefra M, Jorge RMN, Soares CMM. A quasi-3D hyperbolic shear deformation theory for the static and free vibration analysis of functionally graded plates. *Composite Structures*, 2012; 94: 1814–1825.

[27] Neves AMA, Ferreira AJM, Carrera E. A quasi-3D sinusoidal shear deformation theory for the static and free vibration analysis of functionally graded plates. *Composites Part B*, 2012; 43: 711–725.

[28] Sayyad AS, Ghugal YM. Effect of transverse shear and transverse normal strain on the bending analysis of cross-ply laminated beams. *Int J of Applied Mathematics and Mechanics*, 2011; 7: 85–118.

[29] Sayyad AS, Ghugal YM. Flexure of thick beams using new hyperbolic shear deformation theory. *Int J of Mechanics*, 2011;5: 113–122.

[30] Sayyad AS, Ghugal YM, Naik NS. Bending analysis of laminated composite and sandwich beams according to refined trigonometric beam theory. *Curved and Layered Structures*, 2015**;** 2: 279–289.

[31] Sayyad AS, Ghugal YM, Shinde PN. Stress analysis of laminated composite and soft core sandwich beams using a simple higher order shear deformation theory. *J Serbian Society of Compututational Mechanics*, 2015; 9: 15–35.

[32] Carrera E, Giunta G, Petrolo M. **Beam structures***,* John Wiley & Sons, 2011.

[33] Zenkour AM. Maupertuis - Lagrange mixed variational formula for laminated composite structure with a refined higher order beam theory. *Int J Non-Linear Mechanics*, 1997; 32: 989-1001.

[34] Carrera E, Giunta G. Refined beam theories based on a unified formulation. *Int J Applied Mechanics,* 2010; 2: 117-143.

[35] Carrera E, Giunta G, Nali P, Petrolo M. Refined beam elements with arbitrary cross-section geometries. *Computers and Structures*, 2010; 88: 283–93.

[36] Giunta G, Belouettar S, Carrera E. Analysis of FGM beams by means of a unified formulation. *IOP Conference Series: Materials Science and Engineering*, 2010; 10: 1-10.

[37] Thai HT, Vo TP. Bending and free vibration of functionally graded beams using various higher-order shear deformation beam theories. *Int J of Mechanical Sciences*, 2012; 62: 57–66.

[38] Li SR, Batra RC. Relations between buckling loads of functionally graded Timoshenko and homogeneous Euler–Bernoulli beams. *Composite Structures*, 2013; 95: 5–9.

[39] Simsek M. Fundamental frequency analysis of functionally graded beams by using different higher-order beam theories. *Nuclear Engineering and Design*, 2010; **240:** 697–705.

[40] Nguyen TK, Vo TP, Thai HT. Static and free vibration of axially loaded functionally graded beams based on the first-order shear deformation theory. *Composites Part B*, 2013; 55: 147–157.

[41] Hadji L, Daouadji TH, Meziane MAA, Tlidji Y, Bedia EAA. Analysis of functionally graded beam using a new first-order shear deformation theory. *Structural Engineering and Mechanics*, 2016; 57: 315-325.

[42] Hadji L, Khelifa Z, Bedia EAA. A new higher order shear deformation model for functionally graded beams. *KSCE J of Civil Engineering*, 2016; 20(5): 1835-1841.

[43] Bourada M, Kaci A, Houari MSA, Tounsi A. A new simple shear and normal deformations theory for functionally graded beams. *Steel and Composite Structures*, 2015; 18(2): 409-423.

[44] Vo TP, Thai HT, Nguyen TK, Inam F. Static and vibration analysis of functionally graded beams using refined shear deformation theory. *Meccanica*, 2014; 49: 155–168.

[45] Vo TP, Thai HT, Nguyen TK, Maheri A, Lee J. Finite element model for vibration and buckling of functionally graded sandwich beams based on a refined shear deformation theory. *Engineering Structures*, 2014; 64: 12–22.

[46] Sayyad AS, Ghugal YM. A unified shear deformation theory for the bending of isotropic, functionally graded, laminated and sandwich beams and plates. *Int J Applied Mechanics*, 2017; 9: 1-36.

[47] Hebali H, Houari MSA, Tounsi A, Bessaim A, Bedia EEA. A new quasi-3D hyperbolic shear deformation theory for the static and free vibration analysis of functionally graded plates. *ASCE Journal of Engineering Mechanics*, 2014;140:374 – 383.

[48] Bennoun M, Houari MSA, Tounsi A. A novel five variable refined plate theory for vibration analysis of functionally graded sandwich plates. *Mechanics of Advanced Materials and Structures*, 2016;23(4):423 – 431.

[49] Beldjelili Y, Tounsi A, Hassanet S. Hygro-thermo-mechanical bending of S-FGM plates resting on variable elastic foundations using a four-variable trigonometric plate theory Smart Structures and Systems, 2016; 18(4): 755-786.

[50] Bouderba B, Houari MSA, Tounsi A, Mahmoud SR. Thermal stability of functionally graded sandwich plates using a simple shear deformation theory. *Structural Engineering and Mechanics*, 2016;58(3):397-422.

[51] Bousahla AA, Benyoucef S, Tounsi A, Mahmoud SR. On thermal stability of plates with functionally graded coefficient of thermal expansion. *Structural Engineering and Mechanics*, 2016;60(2):313-335.

[52] Boukhari A, Atmane HA, Tounsi A, Bedia EEA, Mahmoud SR. An efficient shear deformation theory for wave propagation of functionally graded material plates. *Structural Engineering and Mechanics*, 2016;57(5):837-859.

[53] Rahmani O, Pedram O. Analysis and modeling the size effect on vibration of functionally graded nanobeams based on nonlocal Timoshenko beam theory. *International Journal of Engineering Science*, 2014; 77: 55-70.

[54] Akgoz B, Civalek O. Bending analysis of embedded carbon nanotubes resting on an elastic foundation using strain gradient theory, *Acta Astronautica*, 2016;119:1–12.

[55] Ebrahimi F, Barati MR. A nonlocal higher-order shear deformation beam theory for vibration analysis of size-dependent functionally graded nanobeams. *Arabian Journal for Science and Engineering*, 2016; 41(5): 1679-1690